

Original citation:

Sierocinski, Pawel, Milferstedt, Kim, Bayer, Florian, Großkopf, Tobias, Alston, Mark, Bastkowski, Sarah, Swarbreck, David, Hobbs, Phil J., Soyer, Orkun S., Hamelin, Jérôme and Buckling, Angus. (2017) A single community dominates structure and function of a mixture of multiple methanogenic communities. *Current Biology*, 27 (21). 3390-3395.e4.

Permanent WRAP URL:

<http://wrap.warwick.ac.uk/95439>

Copyright and reuse:

The Warwick Research Archive Portal (WRAP) makes this work by researchers of the University of Warwick available open access under the following conditions. Copyright © and all moral rights to the version of the paper presented here belong to the individual author(s) and/or other copyright owners. To the extent reasonable and practicable the material made available in WRAP has been checked for eligibility before being made available.

Copies of full items can be used for personal research or study, educational, or not-for-profit purposes without prior permission or charge. Provided that the authors, title and full bibliographic details are credited, a hyperlink and/or URL is given for the original metadata page and the content is not changed in any way.

Publisher's statement:

© 2017, Elsevier. Licensed under the Creative Commons Attribution-NonCommercial-NoDerivatives 4.0 International <http://creativecommons.org/licenses/by-nc-nd/4.0/>

A note on versions:

The version presented here may differ from the published version or, version of record, if you wish to cite this item you are advised to consult the publisher's version. Please see the 'permanent WRAP URL' above for details on accessing the published version and note that access may require a subscription.

For more information, please contact the WRAP Team at: wrap@warwick.ac.uk

1 **A single community dominates structure and function of a mixture of multiple**
2 **methanogenic communities**

3

4 Pawel Sierocinski*^{1,6}, Kim Milferstedt², Florian Bayer¹, Tobias Großkopf³, Mark Alston⁴, Sarah
5 Bastkowski⁴, David Swarbreck⁴, Phil J Hobbs⁵, Orkun S Soyer³, Jérôme Hamelin², Angus
6 Buckling¹

7 ¹ *Biosciences, University of Exeter, Penryn, Cornwall, TR10 9FE, UK*

8 ² *LBE, INRA, 11100, Narbonne, France*

9 ³ *School of Life Sciences, University of Warwick, Coventry, CV4 7AL, UK*

10 ⁴ *Earlham Institute, Norwich Research Park, Norwich, NR4 7UH, UK*

11 ⁵ *Anaerobic Analytics Ltd, Okehampton, EX20 1AS, UK*

12 ⁶ Lead contact

13

14 *Correspondence should be directed to p.sierocinski@exeter.ac.uk

15

16 SUMMARY

17 **The ecology of microbes frequently involves the mixing of entire communities**
18 **(community coalescence), for example flooding events, host excretion and soil tillage**
19 **[1,2], yet the consequences of this process for community structure and function are**
20 **poorly understood [3–7]. Recent theory suggests that a community, due to coevolution**
21 **between constituent species, may act as a partially cohesive unit [8–11], resulting in**
22 **one community dominating following community coalescence. This dominant**
23 **community is predicted to be the one that uses resources most efficiently when grown**
24 **in isolation [11]. We experimentally tested these predictions using methanogenic**
25 **communities, for which efficient resource use, quantified by methane production,**
26 **requires coevolved cross-feeding interactions between species [12]. Following**
27 **propagation in laboratory-scale anaerobic digesters, community composition**
28 **(determined from 16S rRNA sequencing) and methane production of mixtures of**
29 **communities closely resembled that of the single most productive community grown**
30 **in isolation. Analysis of each community's contribution towards the final mixture**
31 **suggests that certain combinations of taxa within a community might be co-selected**
32 **as a result of coevolved interactions. As a corollary of these findings, we also show**
33 **that methane production increased with the number of inoculated communities. These**
34 **findings are relevant to the understanding of the ecological dynamics of natural**

35 **microbial communities, as well as demonstrating a simple method of predictably**
36 **enhancing microbial community function in biotechnology, health and agriculture [13].**

37

38 RESULTS AND DISCUSSION

39 We wanted to determine if coalesced methanogenic communities were dominated by the
40 community that used resources most efficiently in isolation. We used methanogenic
41 communities primarily because methane production is a useful proxy for the ability of an
42 anaerobic community to fully exploit available resources: Methanogenesis results from the
43 conversion of H₂, CO₂ and short chain fatty acids produced by hydrolysis and fermentation of
44 more complex organic material, and is often the only thermodynamically feasible way of
45 actively removing inhibitory end-metabolites [12]. Moreover, methanogenic communities are
46 characterized by complex cross-feeding interactions [12, 14, 15]; hence, the importance of
47 community cohesion in shaping community performance is likely to be particularly important
48 [9]. To provide insight into the temporal dynamics of compositional and functional change
49 following community mixing, we first measured the methane production and composition of
50 two methanogenic communities derived from industrial Anaerobic Digesters (ADs) (Table 1)
51 grown in isolation or as a mixture in laboratory scale ADs. Both the individual communities
52 and mixes were grown in four replicates. To remove any potentially confounding effects
53 caused by differences in starting density of tested communities, we standardized microbial
54 density based on qPCR-estimated counts of 16S rRNA gene copies. We found that the
55 methane production of the mixed community was initially intermediate between the two
56 individual communities, but after 5 weeks propagation started to produce gas at a rate
57 indistinguishable from the more productive of the individual communities (Figure 1A). We
58 examined both the starting point and the endpoint composition of the single and mixed
59 communities by Illumina sequencing 16s rRNA gene amplicon libraries. Consistent with the
60 phenotypic data, the composition of the mixture was much more similar to the better than the
61 worse performing community at the endpoint (Figure 1B). This was despite the single
62 endpoint communities changing considerably from their ancestral composition over the 5
63 weeks (Figure 1B).

64

65 We next determined if a single community dominated when multiple communities were mixed.

66 To this end, we propagated 10 single communities (from either industrial ADs or sewage or
67 agricultural waste AD feedstocks, with each replicated three times), and ten replicates of a
68 mixture of all ten communities (Table 1). The results were consistent with those from the two-
69 community mixture. First, methane production in mixtures of ten communities was higher than
70 the average of the individual communities. However, methane production of the mixtures did
71 not differ from the best performing single community, P13, (Figure 2A), which, like each of the
72 single communities used, was a constituent of all the mixtures. Second, the community
73 composition of mixtures (which varied very little between replicates, presumably because they
74 all had the same 10 community starting inocula) most closely resembled the best performing
75 community, P13 (Figure 2B). More generally, the more compositionally similar an individual
76 community was to the replicated 10-community mixtures, the greater the gas production of
77 the community when grown in isolation (Figure S1). Other community characteristics that
78 positively correlated with methane production were bacterial cell densities and within-
79 community (alpha) diversity, but not methanogen density (Figure S2). In summary, the results
80 demonstrate that the community most efficient at using resources (which in these
81 experiments was also the most diverse) dominates when multiple communities are mixed
82 together, thus enhancing mixed community productivity beyond the average of the
83 component communities.

84

85 We next explored the ecological mechanism(s) underpinning the observed dominance by the
86 community that produced the most methane. One explanation is that multiple taxa from the
87 same community act as semi-cohesive units and are selected together. This might arise as a
88 result of coevolved mutualistic (or unidirectional) cross-feeding interactions, notably between
89 methanogenic Archaea and hydrogen/acetate producers, where each organism both provides
90 essential resources and removes damaging waste products for each other [12,15,16].
91 Moreover, coevolved resource partitioning can result in taxa being selected together, because
92 species are expected to coevolve to minimise competition with co-occurring taxa [17–19].
93 Note that the selection of multiple taxa together in these contexts does not require any form of
94 group selection [11, 20], but simply selection of particular individuals from a key taxon whose
95 presence provides an advantage for individuals from taxa they have coevolved with. This

96 process can be described as ecological co-selection, equivalent to genetic co-selection,
97 where a gene can hitchhike to high frequency purely as consequence of being linked to
98 genes under positive selection [21].

99

100 An alternative explanation is that coevolved interactions within individual communities are
101 relatively unimportant, and the dominant community simply contains more competitive taxa
102 (for any functional task/interaction) than other communities. This does not imply that
103 coevolved cross-feeding interactions are unimportant for methanogenic communities, but that
104 these co-evolved interactions are no more specific for taxa isolated from within a community
105 than taxa isolated from different communities. In other words, functionally equivalent taxa are
106 interchangeable between communities. These different scenarios, selection for the best
107 individual taxa and co-selection, are two extremes of a continuum. The distinction is important
108 because dominance by a single community is necessarily a more likely consequence of
109 community coalescence when co-selection operates. Figure 3 (ABC) provides an illustration
110 of the two extreme scenarios, no co-selection and co-selection of the entire community, and
111 an intermediate case where there are two groups of interacting taxa, or modules, and co-
112 selection occurs within each.

113

114 The most direct way to demonstrate a role of co-selection would be to show that the outcome
115 of competition between single taxa from different communities does not predict the outcome
116 of competition at the community level [11]. Unfortunately, this is not feasible for such complex
117 communities, in which many taxa are very difficult to grow in isolation. However, there are
118 other testable predictions associated with the operation of co-selection or otherwise. If the
119 success of an individual taxon is independent of whether they are in the presence of taxa
120 from the same community (i.e. co-selection does not occur), communities that use resources
121 most efficiently and hence achieve the highest biomass per unit of time (productivity) will
122 contain the highest number of the best-performing taxa. It then follows that there will be a
123 positive relationship between the productivity of a community and the proportion of taxa it
124 contributes to the mixture (Figure 3A). If instead taxa are co-selected as modules, the
125 correlation between individual community contribution and productivity is likely to break down.

126 This is best illustrated by the extreme scenario whereby all taxa within a mixed community
127 are co-selected from a single community: the mixture will be entirely dominated by a single
128 constituent community, hence the contribution of all other communities will be independent of
129 their individual productivity (i.e. they will contribute null to the mixture's composition, even
130 though they have non-zero productivity individually; Figure 3B). The intermediate scenario,
131 where co-selection occurs within two independent modules can also break down this
132 correlation if one module contributes much more to community productivity than the other
133 (Figure 3C).

134

135 To determine if co-selection contributed to our findings, we first estimated the contribution of
136 each community to the 10-community mixtures using a non-negative least squares (NNLS)
137 approach. The community that had the most similar composition to the mixtures (and
138 produced the most methane) contributed an estimated 40% of its taxa to the mixtures, with
139 only two other communities contributing more than 10% of their taxa to the mixtures (Figure
140 3D). We then correlated the contribution each community made to the mixtures with two
141 measures of community productivity: methane production and cell densities (based on 16s
142 rRNA gene copy number), which themselves were positively correlated (Figure S2A). We
143 found no suggestion of a positive correlation between either measure of productivity and
144 contribution to the community (Figure 3D and E). These results suggest that co-selection of
145 taxa played an important role in dominance by the community that produced the most
146 methane.

147

148 That community coalescence results in the most productive individual community dominating
149 the mixed community has direct implications for biotechnological uses of microbial
150 communities. Given that the best performing community in isolation largely determined both
151 the composition and performance of mixtures of communities, methane production should
152 increase with increasing number of communities in a mixture. We therefore inoculated
153 laboratory-scale anaerobic digesters with 1, 2, 3, 4, 6 or 12 communities, ensuring that each
154 of the 12 starting communities was used an equal amount of times at each diversity level
155 ([22]; see Table S1). Cumulative methane production over a five-week period increased with

156 increasing number of communities used as an inoculum (Figure 2C). The positive correlation
157 between community function and the number of inoculating communities is analogous to the
158 commonly observed finding that community productivity increases with increasing species
159 diversity [23]. In this case, the mechanism underlying this positive relationship between the
160 number of communities and productivity is a “sampling effect”: inoculating more communities
161 increases the chance that the best performing community will be present in the mix [24].
162 However, given that domination of mixtures by one community was not complete (Figure 3D
163 and E), it is possible that mixing communities could increase performance beyond that of the
164 maximum of single communities in some circumstances (transgressive over-yielding, [25]).

165

166 Here, we have shown that coalescence of microbial communities results in dominance of a
167 single community, the identity of which can be predicted from its efficiency of resource use in
168 isolation. This dominance is likely to be driven in part by co-selection of interacting taxa within
169 coevolved communities, which is likely to greatly increase the magnitude of dominance
170 following mixing [11]. It is unclear whether such effects would be apparent for aerobic
171 communities where cross-feeding interactions are less important for efficient resource use
172 [26], although studies to date [4] suggest asymmetric outcomes, although less extreme, may
173 be common. Our study has also identified a simple method to significantly improve methane
174 yield during anaerobic digestion: inoculate digesters with a broad range of microbial
175 communities, and the best performing community will dominate. However, further work under
176 a range of conditions is clearly required to determine the generality of these findings. Given
177 that resource use efficiency is often a desirable property of microbial communities, this
178 approach could be applied to a range of biotechnological processes driven by microbial
179 communities, as well as to manipulate microbiomes in clinical and agricultural contexts [13].

180

181 AUTHOR CONTRIBUTIONS

182 Methodology: PS, KM, FB, OSS, PJH, JH, AB; Formal analysis PS, SB, MA and AB;

183 Investigation: PS and FB; Writing - Original Draft: PS and AB; Writing - Review and Edition:

184 All authors; Visualisation PS and AB; Supervision: AB

185

186 ACKNOWLEDGEMENTS

187 The work was funded by the BBSRC, the Royal Society, AXA Research Fund and NERC. KM
188 & JH were funded through the project ENIGME from the INRA metaprogramme MEM (Meta-
189 omics and microbial ecosystems). KM was additionally funded through an Institut Carnot
190 3BCAR international travel grant.

191

192 REFERENCES

- 193 1. Rillig, M.C., Antonovics, J., Caruso, T., Lehmann, A., Powell, J.R., Veresoglou, S.D.,
194 and Verbruggen, E. (2015). Interchange of entire communities: Microbial community
195 coalescence. *Trends Ecol. Evol.* *30*, 470–476.
- 196 2. Rillig, M.C., Lehmann, A., Aguilar-Trigueros, C.A., Antonovics, J., Caruso, T., Hempel,
197 S., Lehmann, J., Valyi, K., Verbruggen, E., Veresoglou, S.D., *et al.* (2016). Soil
198 microbes and community coalescence. *Pedobiologia (Jena)*. *59*, 37–40.
- 199 3. Hausmann, N., and Hawkes, C. (2009). Plant neighborhood control of arbuscular
200 mycorrhizal community composition. *New Phytol.* *183*, 1188–1200.
- 201 4. Livingston, G., Jiang, Y., Fox, J., and Leibold, M. (2013). The dynamics of community
202 assembly under sudden mixing in experimental microcosms. *Ecology* *94*, 2898–2906.
- 203 5. Souffreau, C., Pecceu, B., Denis, C., Rummens, K., and De Meester, L. (2014). An
204 experimental analysis of species sorting and mass effects in freshwater
205 bacterioplankton. *Freshw. Biol.* *59*, 2081–2095.
- 206 6. Adams, H.E., Crump, B.C., and Kling, G.W. (2014). Metacommunity dynamics of
207 bacteria in an arctic lake: The impact of species sorting and mass effects on bacterial
208 production and biogeography. *Front. Microbiol.* *5*.
- 209 7. Calderón, K., Spor, A., Breuil, M.-C., Bru, D., Bizouard, F., Violle, C., Barnard, R.L.,
210 and Philippot, L. (2017). Effectiveness of ecological rescue for altered soil microbial
211 communities and functions. *ISME J.* *11*, 272–283.
- 212 8. Gilpin, M. (1994). Community-level competition: asymmetrical dominance. *Proc. Natl.*
213 *Acad. Sci. U. S. A.* *91*, 3252–3254.
- 214 9. Toquenaga, Y. (1997). Historicity of a simple competition model. *J. Theor. Biol.* *187*,

- 215 175–181.
- 216 10. Wright, C.K. (2008). Ecological community integration increases with added trophic
217 complexity. *Ecol. Complex.* 5, 140–145.
- 218 11. Tikhonov, M. (2016). Community-level cohesion without cooperation. *Elife* 5, e15747.
- 219 12. Schink, B. (1997). Energetics of syntrophic cooperation in methanogenic degradation.
220 *Microbiol. Mol. Biol. Rev.* 61, 262–280.
- 221 13. Rillig, M.C., Tsang, A., and Roy, J. (2016). Microbial community coalescence for
222 microbiome engineering. *Front. Microbiol.* 7, 6–8.
- 223 14. Hillesland, K.L., and Stahl, D. a (2010). Rapid evolution of stability and productivity at
224 the origin of a microbial mutualism. *Proc. Natl. Acad. Sci. U. S. A.* 107, 2124–2129.
- 225 15. Embree, M., Liu, J.K., Al-Bassam, M.M., and Zengler, K. (2015). Networks of energetic
226 and metabolic interactions define dynamics in microbial communities. *Proc. Natl.*
227 *Acad. Sci. U. S. A.* 112, 15450–15455.
- 228 16. Großkopf, T., and Soyer, O. (2016). Microbial diversity arising from thermodynamic
229 constraints. *ISME J.* 10, 2725–2733.
- 230 17. Schluter, D. (2000). The ecology of adaptive radiation.
- 231 18. Roughgarden, J. (1976). Resource partitioning among competing species - A
232 coevolutionary approach. *Theor. Popul. Biol.* 9, 388–424.
- 233 19. MacArthur, R.H. (1970). Species-packing and competitive equilibrium for many
234 species. *Theoretical Popul. Biol.* 1, 1–11.
- 235 20. Gardner, A., and Grafen, A. (2009). Capturing the superorganism: a formal theory of
236 group adaptation. *J. Evol. Biol.* 22, 659–671.
- 237 21. Baker-Austin, C., Wright, M.S., Stepanauskas, R., and McArthur, J. V. (2006). Co-
238 selection of antibiotic and metal resistance. *Trends Microbiol.* 14, 176–182.
- 239 22. Hodgson, D.J.D., Rainey, P.B., and Buckling, A. (2002). Mechanisms linking diversity,
240 productivity and invasibility in experimental bacterial communities. 269, 2277–2283.
- 241 23. Tilman, D., and Lehman, C. (1997). Plant diversity and ecosystem productivity:
242 theoretical considerations. *Proc. Natl. Acad. Sci. U. S. A.* 94, 1857–1861.
- 243 24. Tilman, D. (1999). The ecological consequences of changes in biodiversity: A search
244 for general principles. In *Ecology* (Ecological Society of America), pp. 1455–1474.

- 245 25. Harper, D. (1977). *The population biology of plants* (Academic Press).
- 246 26. Morris, B.E.L., Henneberger, R., Huber, H., and Moissl-Eichinger, C. (2013). Microbial
247 syntrophy: Interaction for the common good. *FEMS Microbiol. Rev.* 37, 384–406.
- 248 27. Einen, J., Thorseth, I.H., and Øvreås, L. (2008). Enumeration of Archaea and Bacteria
249 in seafloor basalt using real-time quantitative PCR and fluorescence microscopy.
250 *FEMS Microbiol. Lett.* 282, 182–187.
- 251 28. Ruijter, J.M., Ramakers, C., Hoogaars, W.M.H., Karlen, Y., Bakker, O., van den hoff,
252 M.J.B., and Moorman, A.F.M. (2009). Amplification efficiency: Linking baseline and
253 bias in the analysis of quantitative PCR data. *Nucleic Acids Res.* 37, e45.
- 254 29. Brankatschk, R., Fischer, T., Veste, M., and Zeyer, J. (2013). Succession of N cycling
255 processes in biological soil crusts on a Central European inland dune. *FEMS*
256 *Microbiol. Ecol.* 83, 149–160.
- 257 30. Kozich, J.J., Westcott, S.L., Baxter, N.T., Highlander, S.K., and Schloss, P.D. (2013).
258 Development of a dual-index sequencing strategy and curation pipeline for analyzing
259 amplicon sequence data on the MiSeq Illumina sequencing platform. *Appl. Environ.*
260 *Microbiol.* 79, 5112–5120.
- 261 31. Eren, A.M., Maignien, L., Sul, W.J., Murphy, L.G., Grim, S.L., Morrison, H.G., and
262 Sogin, M.L. (2013). Oligotyping: differentiating between closely related microbial taxa
263 using 16S rRNA gene data. *Methods Ecol. Evol.* 4, 1111–1119.
- 264 32. Caporaso, J.G., Kuczynski, J., Stombaugh, J., Bittinger, K., Bushman, F.D., Costello,
265 E.K., Fierer, N., Peña, A.G., Goodrich, J.K., Gordon, J.I., *et al.* (2010). QIIME allows
266 analysis of high-throughput community sequencing data. *Nat. Methods* 7, 335–336.
- 267 33. Edgar, R.R.C. (2010). Search and clustering orders of magnitude faster than BLAST.
268 *Bioinformatics* 26, 2460–2461.
- 269 34. Edgar, R.C., Haas, B.J., Clemente, J.C., Quince, C., and Knight, R. (2011). UCHIME
270 improves sensitivity and speed of chimera detection. *Bioinformatics* 27, 2194–2200.
- 271 35. McDonald, D., Price, M.N., Goodrich, J., Nawrocki, E.P., DeSantis, T.Z., Probst, A.,
272 Andersen, G.L., Knight, R., and Hugenholtz, P. (2012). An improved Greengenes
273 taxonomy with explicit ranks for ecological and evolutionary analyses of bacteria and
274 archaea. *ISME J.* 6, 610–8.

- 275 36. Mullen, K., and Van Stokkum, I. (2007). The Lawson-Hanson algorithm for non-
276 negative least squares (NNLS).
- 277 37. Soetaert, K., Meersche, K.V.D., and Oevelen, D. V (2009). Package limSolve, solving
278 linear inverse models in R.

279

280 FIGURE LEGENDS

281 **Figure 1: Temporal dynamics of methane production and composition when two**
282 **communities are mixed.** A) Cumulative methane production in ml (\pm SEM) over time of:
283 community P01 (white circles), community P05 (black circles) and their mixes (grey circles).
284 Cumulative methane production differed between treatments (ANOVA: $F_{2,9} = 23.2$, $P <$
285 0.001), but did not differ between the mixed community and P05 (Tukey-Kramer HSD: $P =$
286 0.5). P01 was lower than both other treatments (Tukey-Kramer HSD: $P < 0.001$ in both
287 cases). B) NMDS plot of unweighted UniFrac of communities P01 (white), P05 (black) and
288 their mixes (grey). Ancestral samples are represented by squares with samples from the
289 endpoint of the experiment by circles. At the endpoint, P05 was compositionally more similar
290 to the mixtures than P01, based on both unweighted (t -tests of mean distance to each mixture
291 for each replicate single community: $t_6 = 8.3$, $P < 0.001$) and weighted ($t_6 = 2.3$, $P = 0.03$)
292 UniFrac distances.

293

294 **Figure 2: Methane production and community composition when multiple communities**
295 **are mixed.** A) Total methane production of mixed (grey) and individual communities (white),
296 with mean values shown as horizontal lines. Mean total methane production was greater for
297 mixtures than for individual communities (t -test: $P < 0.001$ in 9 cases), except when measured
298 against community P13 (the best performer). B) NMDS plot of unweighted unifrac of 10
299 mixtures (grey) and 9 individual communities (white). Numbers in circles refer to individual
300 community identifiers (Table 1). Community P13 was significantly closer in composition to the
301 10 mixed communities than any other community (weighted and unweighted UniFrac
302 distances; Paired t -tests; $P < 0.001$, in all cases). There was also a significant link between
303 the community composition and the difference in gas production between the communities
304 (see Figure S1). Note: DNA yield from community P06, which had the lowest gas production

305 of all communities, was insufficient for sequencing, therefore it is excluded from this and
306 following graphs. C) Individual communities (white circles) and their average methane
307 production (white line); mixes of communities (grey circles) and their averages (grey line).
308 There was a monotonic increase in methane production with number of communities used
309 (Regression: $F_{1,26} = 5.4$, $P = 0.03$). For community composition of the mixes, see Table 1 and
310 Table S1.

311

312

313 **Figure 3: The role of co-selection in explaining dominance by a single community.** A-C)

314 The top panels illustrate three hypothetical scenarios describing how communities contribute
315 to a mixture of communities, while the bottom panels show the expected relationships
316 between a community's contribution and its methane production. The letters within the top
317 panels indicate taxa that drive two biochemical processes (abcd and ef); capitalised letters
318 are the best representatives of a taxon among all the communities. A). No co-selection. B).
319 Co-selection of all taxa within a community. C). Co-selection of taxa within two independent
320 modules. D). Mean estimated relative contribution of each individual community (numbered)
321 towards the 10 coalesced communities calculated using the NNLS method, plotted against
322 mean cumulative methane production for each community; there is no significant relationship
323 (Regression; $F_{1,7} = 1.7$, $P > 0.2$). E) As D, but relative contribution is plotted against number of
324 bacterial and archaeal cells calculated based on the 16S rRNA gene copy number
325 (Regression; $F_{1,7} = 1.7$, $P > 0.5$. Note the relative contribution is not a fractional contribution
326 because some OTUs present in the mixture were not detected in the constituent
327 communities. This is presumably because they only reached detected frequencies in the
328 mixture, but we can't rule out that the community that we failed to get sufficient reads from
329 contributed to the composition of the mixtures. Mind that the cell densities of Archaea and
330 bacteria do not significantly correlate with the gas production (see Figure S2).

331

332 Table 1: **List of individual communities used in this analysis and their source.** All

333 Anaerobic Digester (AD) communities were derived from industrial ADs in the South West of

334 England. Specific locations cannot be provided because of commercial sensitivity. Note that
335 experiment numbers correspond with figure numbers.

336

Sample name	Feed/Type	Temperature	Used in experiments
P01	Silage and Foodwaste Anaerobic Digester (AD)	44 - 42.5°C	1,2,3
P02	Silage + Food waste AD	44 - 42.5°C	2,3
P03	Maize/Cow Slurry/Chicken Manure AD	45°C	3
P04	Maize/Cow Slurry/Chicken Manure AD	45°C	2,3
P05	Sewage Sludge AD	36°C	1,2,3
P06	Raw Sewage	Ambient	2,3
P08	Thickened Sewage Sludge	Ambient	2,3
P09	Sewage Based AD	36°C	2,3
P10	Food Waste AD	36°C	2,3
P11	Cow Slurry	Ambient	3
P12	Silage, Slurry and Manure Pre-Digestate	Ambient	3
P13	Silage, Slurry and Manure AD	40°C	2,3
P15	Food waste AD	36°C	2

337

338

339

340

341 STAR METHODS

342 **CONTACT FOR REAGENT AND RESOURCE SHARING**

343

344 The authors are happy to share any further resources linked to the research involved with
345 qualified third parties. Further information and requests for resources and reagents should be
346 directed to and will be fulfilled by the Lead Contact, Pawel Sierocinski
347 (p.sierocinski@exeter.ac.uk).

348

349 **EXPERIMENTAL MODEL AND SUBJECT DETAILS**

350

351 **Methanogenic communities**

352 The communities used were collected from anaerobic digesters (AD plants: communities
353 P01,P02, P03, P04, P05, P09, P10, P13 and P15) and communities present in nature used to
354 seed the AD plants (communities P06, P08, P11, P12, see the details in Table 1). All the
355 communities have been collected in the South West area of United Kingdom from operating
356 Anaerobic Digesters and the seeding communities they use for the reactors. The

357 communities were operating at temperatures between ambient and 45°C in their places of
358 origin. Communities were stored at 4°C prior to use.

359

360 **METHOD DETAILS**

361

362 **Cultivation details**

363 For all experiments, communities were grown in 500 ml bottles (600ml total volume with
364 headspace; Duran) using the commercially available Automated Methane Potential Test
365 System (AMPTS, Bioprocess Control Sweden AB) to measure CO₂-stripped biogas
366 production (referred to as methane in this paper). Samples were fed weekly with 25 ml of
367 defined medium in a fed-batch mode using a defined medium (see below for media
368 composition).

369

370 The communities used in experiment 1 were equalised in terms of bacterial cells per gram of
371 sample before inoculation using M9 salts to dilute them to the community with the lowest cell
372 density, based on qPCR enumeration of 16S rRNA gene copies. For experiments 2 and 3,
373 starting 16S rRNA copy number was determined (but not equalised between communities)
374 and did not correlate with methane production. The fermenters were inoculated with 275 g of
375 sample and fed with 25 ml of defined medium: meat extract 111.1 g l⁻¹, cellulose 24.9 g l⁻¹,
376 starch 9.8 g l⁻¹ glucose 0.89 g l⁻¹, xylose 3.55 g l⁻¹ (carbon to nitrogen ratio of 15:1) every week,
377 starting with t₀. Before the start of the fermentation, 0.3 mL of 1000x Trace Metal stock (1 g l⁻¹
378 FeCl₂ · 4H₂O, 0.5 g l⁻¹ MnCl₂ · 4H₂O, 0.3 g l⁻¹ CoCl₂ · 4H₂O, 0.2 g l⁻¹ ZnCl₂, 0.1 g l⁻¹ NiSO₄ ·
379 6H₂O, 0.05 g l⁻¹ Na₂MoO₄ · 4H₂O, 0.02 g l⁻¹ H₃BO₃, 0.008 g l⁻¹ Na₂ WO₄ · 2H₂O, 0.006 g l⁻¹
380 Na₂SeO₃ · 5H₂O, 0.002 g l⁻¹ CuCl₂ · 2H₂O) was added to each fermenter.

381

382 **Experiment structure**

383 In Experiment 1 (results shown in Figure 1) we cultivated community P01 (four replicates) and
384 community P05 (four replicates) and a 1:1 mix of the two. It ran for 5 weeks before samples
385 were harvested for sequencing (see below). The initial community was sequenced at the
386 same time. In Experiment 2 (results shown in Figure 2), we cultivated 10 individual

387 communities (listed in Table 1), in triplicate, and 10 mixes of all 10 communities mixed in
388 equal volumes, at the same total volume as the single communities. After 6 weeks samples
389 were harvested for sequencing. In Experiment 3 (results shown in Figure 2C) we used 12
390 communities (detailed in Table 1). They were grown in isolation as well as pseudo-randomly
391 combined to create a gradient of number of starting communities, with each community used
392 only once for each number of communities. This resulted in 12 single communities, 6 pairs, 4
393 triplets, 3 quadruplets, 2 mixes of 6 and one mix of 12 communities. Specific details of mixing
394 can be seen in Table S1. The cultures were propagated for 5 weeks.

395

396 **Measuring methane content of Biogas**

397 All resulting lab-scale reactors inoculated with the samples were run at 37°C using the
398 Automatic Methane Potential Test System (AMPTS). The AMPTS is a setup of 15 simple
399 fermenters using a 0.5L lab bottle as the vessel with its own stirring system provided with a
400 butyl rubber stopper and sampling ports. It is connected to an online gas measuring system to
401 allow continuous gas measurements. The AMPTS system measures the volume of biogas
402 produced following stripping of CO₂ (by passing the gas through 50 ml of 3M NaOH solution)
403 from the produced gas. To reproduce our results, however, there is no need for a
404 sophisticated setup, some pilot experiments yielding similar results in terms of gas production
405 were conducted using anaerobic serum flasks. We confirmed that the measured biogas was
406 >95% methane using Gas Chromatography with Flame Ionisation Detection optimized for
407 methane detection.

408

409 **DNA extraction and qPCR quantification**

410 DNA for 16S rRNA gene amplicon sequencing was extracted using QIAamp DNA Stool Mini
411 Kit (QIAGEN) or FastDNA™ SPIN Kit for Soil (MP), depending on the experiment. Note that
412 DNA extraction for mixed community P06 from experiment 2 failed. The DNA for qPCR was
413 extracted with the QIAamp DNA Stool Mini Kit (QIAGEN), protocol for pathogen detection
414 with the 95°C incubation step and the Powerlyzer Powersoil DNA KIT (MOBIO). DNA from
415 *Acinetobacter baylyi*, *Pseudomonas fluorescens* SBW25 for Bacteria and from *Halobacterium*
416 *salinarum* DSM 669 for Archaea was used as standards. The primers [27] used to quantify

417 Bacteria were 16S rRNA 338f - ACT CCT ACG GGA GGC AGC AG, 518r - ATT ACC GCG
418 GCT GCT GG for Archaea: 931f - AGG AAT TGG CGG GGG AGC A, m1100r - BGG GTC
419 TCG CTC GTT RCC. The reagents used were: 1x Brilliant III Ultra-Fast SYBR® Green QPCR
420 Master Mix; 150nM 338f and 300nM 518r or 300nM 931f and 300 nM m1100r; ROX 300nM;
421 and BSA 100 ng/μl final concentration. All samples were run in triplicate on a StepOnePlus
422 (Applied Biosystems) qPCR machine using a program with 3 minutes 95°C initial denaturation
423 followed by 40 cycles of 5 seconds at 95°C and 10 seconds at 60°C, followed by a melting
424 curve 95°C for 15 seconds; 60°C for 1 minute ramping up to 95°C in steps of 0.3°C for 15
425 seconds each. The melting curve analysis and the confirmation of the negative controls was
426 done using StepOne Software v.2.3 (life technologies). The Cq values and the efficiencies of
427 the samples and standards was determined as previously using LinRegPCR version
428 2016.0[28]. The quantities were calculated using the one point calibration method as
429 described earlier[29].

430

431 **Amplicon library construction and sequencing**

432 16S rRNA gene libraries were constructed using primers designed to amplify the V4 region
433 and multiplexed [30]. Amplicons were generated using a high-fidelity polymerase (Kapa 2G
434 Robust) and purified using the Agencourt AMPure XP PCR purification system and quantified
435 using a fluorometer (Qubit, life technologies). The purified amplicons were then pooled in
436 equimolar concentrations by hand based on Qubit quantification. The resulting amplicon
437 library pool was diluted to 2 nM with sodium hydroxide and 5 μl transferred into 995 μl HT1
438 (Illumina) to give a final concentration of 10 pM. 600 μl of the diluted library pool was spiked
439 with 10% PhiX Control v3 and placed on ice before loading into Illumina MiSeq cartridge
440 following the manufacturer's instructions. The sequencing chemistry utilised was MiSeq
441 Reagent Kit v2 (500 cycles) with run metrics of 250 cycles for each paired end read using
442 MiSeq Control Software 2.2.0 and RTA 1.17.28.

443

444 **Analyses of sequenced samples**

445 MiSeq amplicon reads were merged using Illumina-utils software [31]. We quality-filtered only
446 the mismatches in the overlapping region between read pairs using a minimum overlap (--

447 min-overlap-size) of 200 nt and a minimum quality Phred score (--min-qual-score) of Q20. We
448 allowed no more than five mismatches per 100 nt (-P 0.05) over the 200 nt overlapping
449 region.

450

451 Reads that fulfilled the quality criteria were analysed using Quantitative Insights Into Microbial
452 Ecology (QIIME v.1.7) [32]. We removed chimera using the *identify_chimeric_seqs.py* script,
453 UCHIME reference 'Gold' database and USEARCH [33,34], which we also used to select
454 OTUs. We assigned the taxonomy of our reads with QIIME *pick_open_reference_otus.py*
455 function, using the Greengenes database version v13_8[35] as a reference with a minimum
456 cluster size of 2 (i.e., each OTU must contain at least two sequences). We collapsed the
457 technical replicates and filtered out the low abundance OTUs (<0.01% total,
458 *filter_otus_from_otu_table.py*) and samples rarefied to an even depth of 26702 for both
459 experiments where sequencing data is available. QIIME was used to calculate alpha and beta
460 diversity data and produce NMDS plots.

461

462 **QUANTIFICATION AND STATISTICAL ANALYSIS**

463 MacQIIME was used to calculate alpha and beta diversity data and produce NMDS plots.
464 Data obtained with MacQIIME was later combined with the gas production data and analysed
465 using JMP Pro 13 software (SAP) as described in the Figure legends.

466

467 For the NNLS analysis, following removal of low abundance OTUs and cumulative sum
468 scaling transformation, the resulting biom file was used to create a matrix $A \in \mathbb{Z}_{\geq 0}^{m \times n}$ (m rows
469 of OTUs by n sample columns) for all of the single communities, and a column vector $b \in \mathbb{Z}_{\geq 0}^m$
470 for each of the mixed communities; both A and b hold non-negative integers of OTU
471 abundances. Note that one of the individual samples contained a negligible number of reads
472 and was discarded from the analysis. The contribution, or weight, of each seed sample to the
473 pattern of OTUs observed in each of the mixed communities is given by the column vector $x \in$
474 \mathbb{R}^n when solving a system of linear equations $Ax = b$. Written out this equation ($Ax = b$)
475 looks like this for each mixture:

476

477

$$478 \begin{pmatrix} \text{OTU}_{1,S1} & \cdots & \text{OTU}_{1,Sn} \\ \vdots & \ddots & \vdots \\ \text{OTU}_{m,S1} & \cdots & \text{OTU}_{m,Sn} \end{pmatrix} \mathbf{x} \begin{pmatrix} x_{S1} \\ \vdots \\ x_{Sm} \end{pmatrix} = \begin{pmatrix} \text{OTU}_{mix_1} \\ \vdots \\ \text{OTU}_{mix_m} \end{pmatrix}$$

479

480

481 where S refers to each single community.

482

483

484

485

486

487

488

489

490

491

492

493

494

495

496 DATA AND SOFTWARE AVAILABILITY

497

498 The raw sequences obtained from our experiments are available at the European Nucleotide

499 Archive and may be accessed at <http://www.ebi.ac.uk/ena/data/view/PRJEB21193>

500 (Experiment 1) and <http://www.ebi.ac.uk/ena/data/view/PRJEB21187> (Experiment 2). We also

501 included the R code that allows the user to calculate the contribution a single community has

502 in a mix of communities (see Method S1). Using this code, a NNLS analysis can be

503 conducted with the input of a pre-filtered OTU table.

504

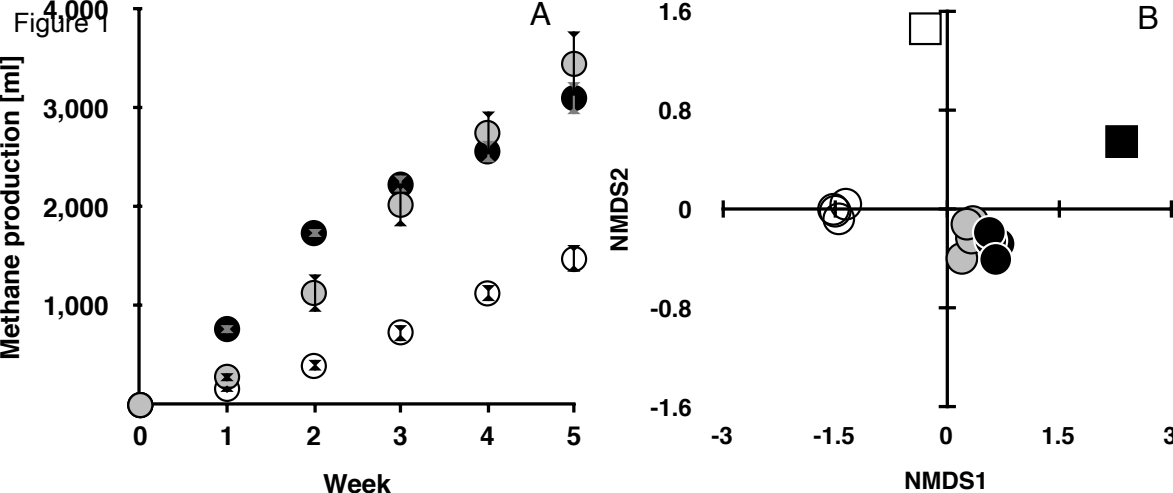
505

KEY RESOURCES TABLE

REAGENT or RESOURCE	SOURCE	IDENTIFIER
Antibodies		
Bacterial and Virus Strains		
Biological Samples		
Chemicals, Peptides, and Recombinant Proteins		
Brilliant III Ultra-Fast SYBR (R) Green QPCR Master Mix	Agilent Technologies	600882-51
meat extract	Sigma-Aldrich Co. LLC.	70164-500G
Xylose	Sigma-Aldrich Co. LLC.	W360100-1KG
Cellulose	Sigma-Aldrich Co. LLC.	C6288
Starch	Sigma-Aldrich Co. LLC.	33615-1KG
Glucose	Sigma-Aldrich Co. LLC.	G8270-1KG
Critical Commercial Assays		
QIAamp DNA Stool Mini Kit (QIAGEN)	Qiagen	ID: 51504
FastDNA™ SPIN Kit for Soil	MP Biomedicals, LLC	116560200
PowerLyzer® PowerSoil® DNA Isolation Kit	MO BIO Laboratories, Inc.	12855-100
Deposited Data		
Sequencing data Experiment 1	European Nucleotide Archive	http://www.ebi.ac.uk/ena/data/view/PRJEB21193

Sequencing data Experiment 2	European Nucleotide Archive	http://www.ebi.ac.uk/ena/data/view/PRJEB21187
Experimental Models: Cell Lines		
Experimental Models: Organisms/Strains		
Community P01	Silage and Foodwaste Anaerobic Digester (AD)	This paper
Community P02	Silage + Food waste AD	This paper
Community P03	Maize/Cow Slurry/Chicken Manure AD	This paper
Community P04	Maize/Cow Slurry/Chicken Manure AD	This paper
Community P05	Sewage Sludge AD	This paper
Community P06	Raw Sewage	This paper
Community P08	Thickened Sewage Sludge	This paper
Community P09	Sewage Based AD	This paper
Community P10	Food Waste AD	This paper
Community P11	Cow Slurry	This paper
Community P12	Silage, Slurry and Manure Pre-Digestate	This paper
Community P13	Silage, Slurry and Manure AD	This paper
Community P15	Food waste AD	This paper
Oligonucleotides		
338f - ACT CCT ACG GGA GGC AGC AG	[27]	
518r - ATT ACC GCG GCT GCT GG	[27]	
931f - AGG AAT TGG CGG GGG AGC A	[27]	
m1100r - BGG GTC TCG CTC GTT RCC	[27]	
Recombinant DNA		
Software and Algorithms		

StepOne Software v.2.3	life technologies	https://www.thermofisher.com/uk/en/home/technical-resources/software-downloads/StepOne-and-StepOnePlus-Real-Time-PCR-System.html#
LinRegPCR version 2016.0	[28]	linregpcr.nl
R version 3.4.0	R Core Team (2013).	Mac: https://cran.r-project.org/bin/macosx/ PC: https://cran.r-project.org/bin/windows/base/old/
macQIIME	[32]	http://www.wernerlab.org/software/macqiime/download
Other		
NNLS Method for assessing community contribution in a mix	This paper,	Method S1



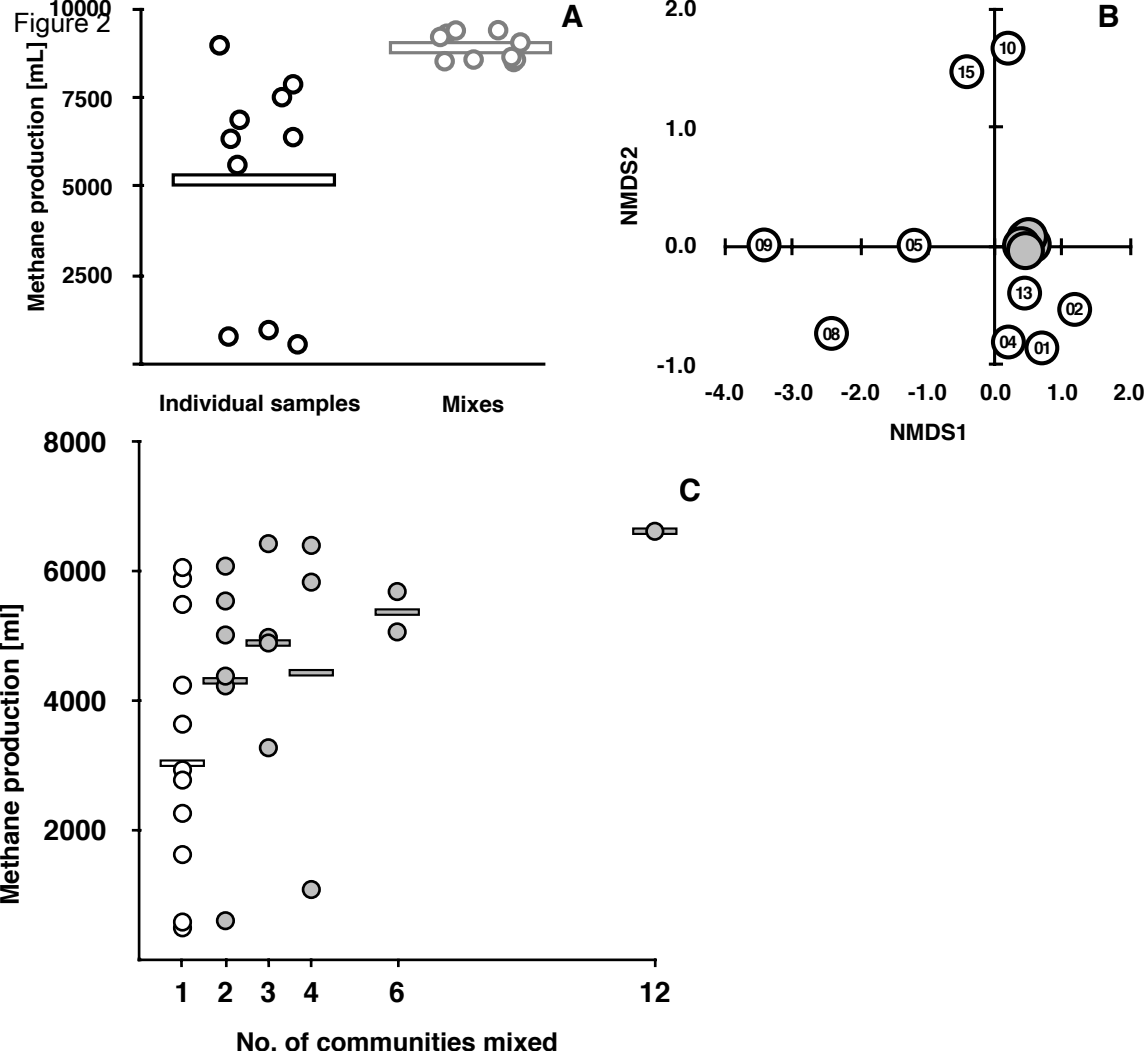
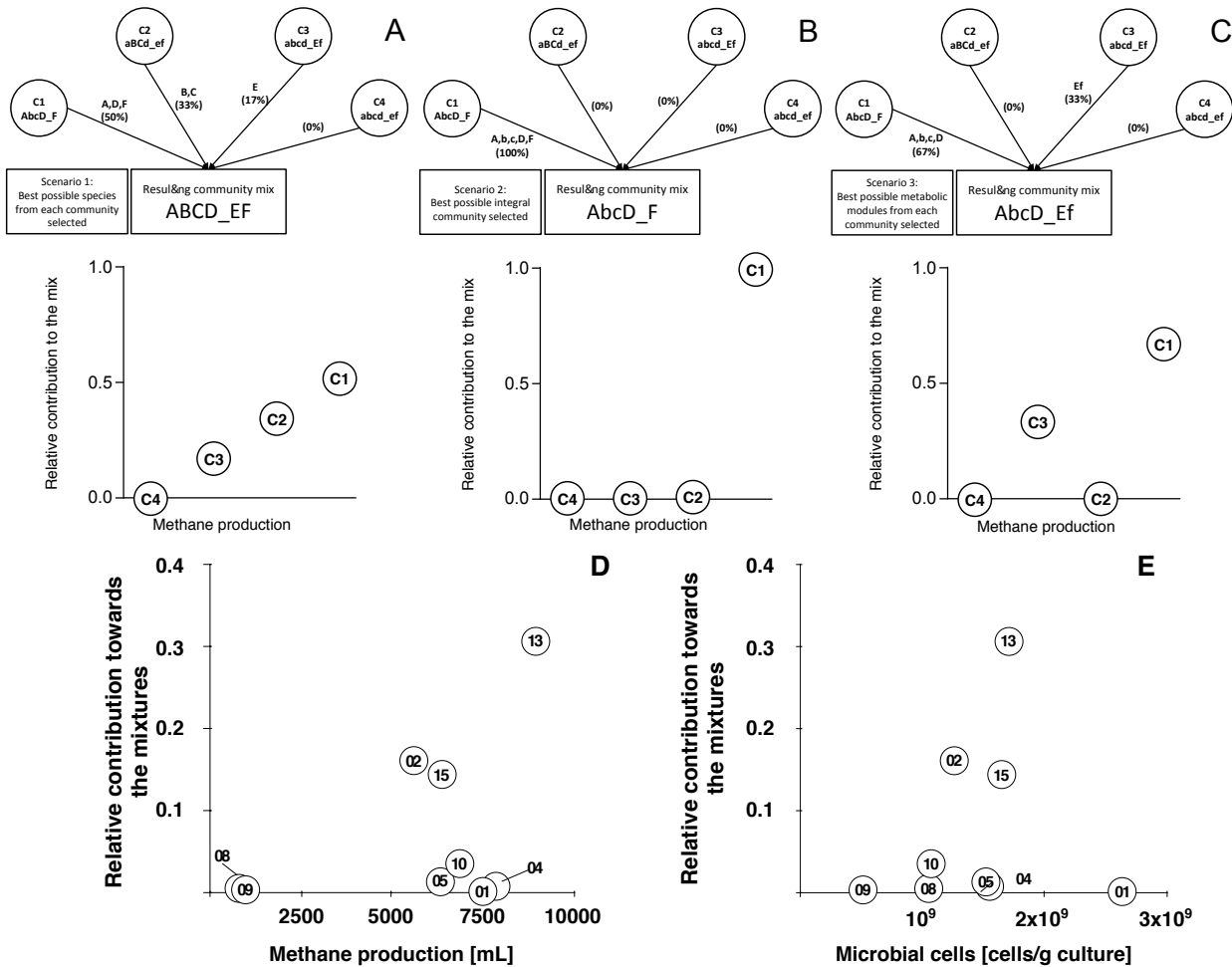


Figure 3



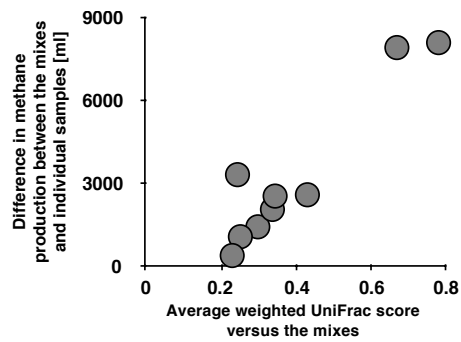


Figure S1: The relationship between the difference in composition of single communities from the mixtures and the difference in gas production of single communities from the mixture related to Figures 2A, 2B.. The Y-axis shows the difference in gas production between the mean of three replicates of each individual community and the mean gas production of the mixes (the smaller the value, the more similar the gas production to the mixtures). The X-axis shows the mean unweighted UniFrac distance between individual communities and each of the ten mixtures (the smaller the value, the more similar the community composition to the mixtures). These two variables are positively correlated (Spearman $\rho = 0.86$, $P < 0.001$). Qualitatively similar results were obtained using weighted UniFrac distances (Spearman $\rho = 0.75$, $P < 0.02$).

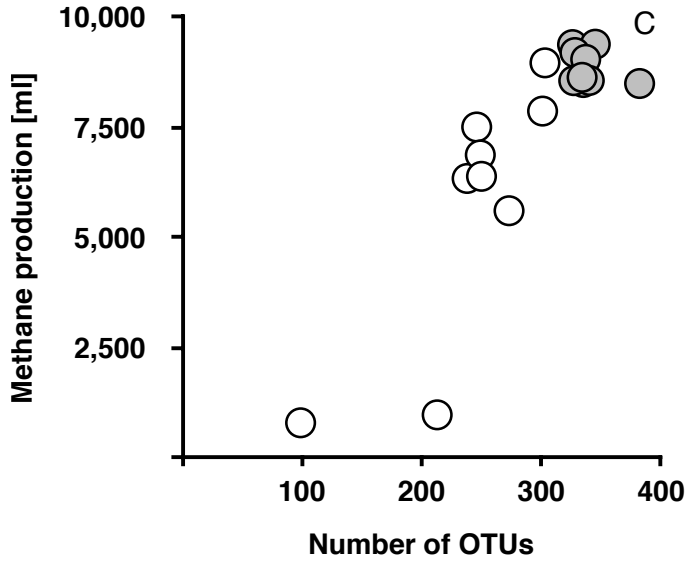
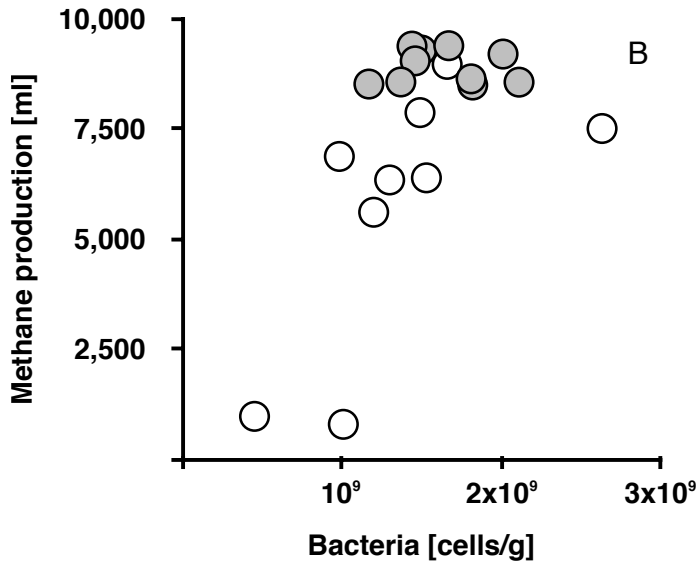
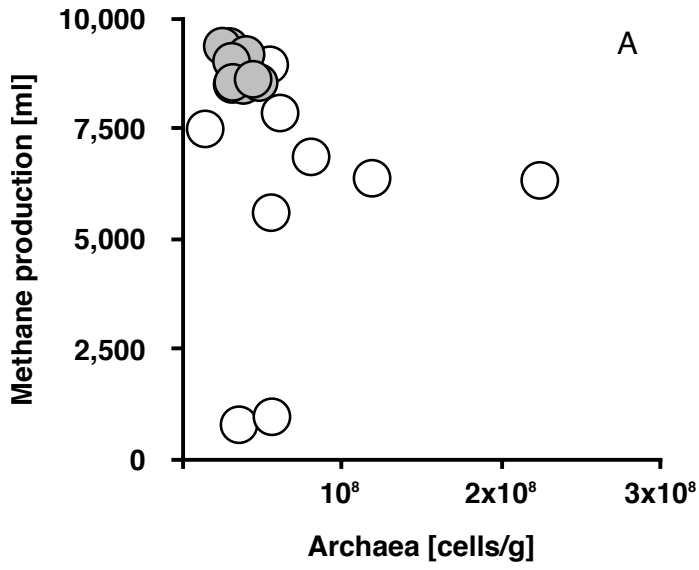


Figure S2: Within-community predictors of methane production from Experiment 2 related to Figure 3D, 3E. Relationships between methane production [ml] and: A) Archaeal densities [\log_{10} cells/g] (Regression: $F_{1,15} = 0.32$, $P > 0.2$); B) Bacterial densities [\log_{10} cells/g] (Regression: $F_{1,16} = 16.5$, $P < 0.001$); and C) number of OTUs (Regression: $F_{1,16} = 51.6$, $P < 0.001$). The reported statistics are based on combined mixed (grey circles) and individual (white circles) communities, but the same qualitative relationships were found when mixed communities were excluded from the analyses (Archaeal density: $F_{1,7} = 0.07$, $P > 0.2$; Bacterial density: $F_{1,7} = 92$, $P < 0.02$; OTUs: $F_{1,7} = 16.4$, $P < 0.01$).

Sample consisting of community(ies)	No. of communities in the mix	Gas production after 4 weeks	Gas production of the best component of the mix after 4 weeks	Average gas production of all components of a mix after 4 weeks	Difference in gas production between a mix and its best component	Difference in gas production between a mix and the average of its components
P06	1	494.9	N/A	N/A	N/A	N/A
P08	1	584.3	N/A	N/A	N/A	N/A
P09	1	600.8	N/A	N/A	N/A	N/A
P12	1	1626.2	N/A	N/A	N/A	N/A
P11	1	2262.8	N/A	N/A	N/A	N/A
P03	1	2776.8	N/A	N/A	N/A	N/A
P01	1	2935.5	N/A	N/A	N/A	N/A
P02	1	3640.8	N/A	N/A	N/A	N/A
P05	1	4243.0	N/A	N/A	N/A	N/A
P10	1	5490.1	N/A	N/A	N/A	N/A
P04	1	5891.3	N/A	N/A	N/A	N/A
P13	1	6060.3	N/A	N/A	N/A	N/A
P01+P11	2	4231.70	2935.50	2599.15	1296.20	1632.55
P02+P09	2	5018.40	3640.80	2120.80	1377.60	2897.60
P12+P03	2	604.70	2776.80	2201.50	-2172.10	-1596.80
P08+P05	2	4383.00	4243.00	2413.65	140.00	1969.35
P04+P06	2	5543.40	5891.30	3193.10	-347.90	2350.30
P13+P10	2	6081.40	6060.30	5151.65	21.10	929.75
P03+P12+P01	3	3276.30	2935.50	2446.17	340.80	830.13
P08+P02+P06	3	4980.60	3640.80	1573.33	1339.80	3407.27
P04+P11+P13	3	6429.10	6060.30	4738.13	368.80	1690.97
P05+P09+P10	3	4894.80	5490.10	3444.63	-595.30	1450.17
P01+P13+P10+P05	4	5834.60	6060.30	4682.23	-225.70	1152.38
P02+P04+P11+P06	4	6401.90	5891.30	3072.45	510.60	3329.45
P03+P08+P09+P12	4	1086.50	2776.80	1397.03	-1690.30	-310.53
P12+P02+P01+P09	6	5065.90	4243.00	2271.77	822.90	2794.13

+P08+P05						
P03+P04+P06+P10 +P11+P13	6	5689.20	6060.30	3829.37	-371.10	1859.83
All 12 communities' mix	12	6620.00	6060.30	3050.57	559.70	3569.43
AVERAGE FOR ALL MIXES		4758.8	4672.9	3011.6	85.9	1747.2

Table S1: Community mixing setup and detailed results of Experiment 3 related to Figure 2C. The details of the communities used can be found in Table 1.

Method S1:

```
#####
## Solving a system of linear equations for a non-square [m > n] ##
## matrix via the use of non-negative least squares [NNLS]. ##
## Return the solution 'weights' and residual sum of squares. ##
## ##
## Mark Alston, Earlham Institute: mark.alston@earlham.ac.uk ##
#####

## ===== ##
## Install the R packages phyloseq, biomformat, nnlS and limSolve.
## Now load as required...
## ===== ##

library("phyloseq")
packageVersion("phyloseq")

library("biomformat")
packageVersion("biomformat")

library("nnlS")
packageVersion("nnlS")

## ===== ##
## READ IN THE OTU table
## ===== ##
## MAPPING FILE TO BE USED: 'mappingFile.txt'
## OTU TABLE TO BE USED: 'CSS_norm_rawValues.biom'

## SET YOUR WORKING DIRECTORY, e.g. point to where your files are located
setwd("/path/to/the/data")

## Quick look at the OTU table which is in biom format
read_biom("CSS_norm_rawValues.biom")

## load the biom file into phyloseq
data = import_biom("CSS_norm_rawValues.biom")
data

## ===== ##
## Give meaningful names to the Taxon Column Headers and create a phyloseq object
## ===== ##
myTaxTable <- tax_table(data)
colnames(myTaxTable) <- c("Kingdom", "Phylum", "Class", "Order", "Family", "Genus", "Species")

### take a look ###
head(myTaxTable)
rank_names(myTaxTable)

OTU = otu_table(data)
TAX = tax_table(myTaxTable)

myPhyloSeq_allData <- phyloseq(OTU, TAX)
myPhyloSeq_allData

## ===== ##
## Incorporate some metadata about the samples ### i.e. first create a mappingFile.txt in a text editor
## ===== ##
SAMPLES = import_qiime_sample_data("mappingFile.txt")
class(SAMPLES)

## ===== ##
## MERGE the bits and bobs into a new phyloseq object
## ===== ##
myPhyloSeq <- merge_phyloseq(myPhyloSeq_allData, SAMPLES)
myPhyloSeq

## inspect the OTU table
otu_table(myPhyloSeq)

## Checking the column headers and looking at the mapping file we see that
## columns 3,2,1,6,18,17,4,7,5 correspond to the 9 SINGLE communities [SAM11640-SAM11649]
## columns 11,12,10,19,15,16,13,14,8,9 correspond to the 10 MIXED communities [SAM11630-SAM11639]

## ===== ##
## collapse OTU table at the 'family' level, and generate matrix 'A' [A.X = b]
## ===== ##

bacteria_family <- tax_glom(myPhyloSeq, taxrank="Family")
bacteria_family_df <- as.data.frame(get_taxa(otu_table(bacteria_family)) )
bacteria_family_singleComm_df <- bacteria_family_df[,c(3,2,1,6,18,17,4,7,5)]

row.names(bacteria_family_singleComm_df) <- NULL
colnames(bacteria_family_singleComm_df) <- NULL
```

```

## ===== ##
## get matrix 'A'
## ===== ##
bacteria_family_matrix_A <- as.matrix(bacteria_family_singleComm_df)

## ===== ##
## get vector 'b' [A.X = b], one for each of the 'mixed' samples [OTU table columns 11,12,10,19,15,16,13,14,8,9]
## ===== ##
b_M01_bac_family_df <- bacteria_family_df[,c(11)]
bf_M01 <- as.matrix(b_M01_bac_family_df)

b_M02_bac_family_df <- bacteria_family_df[,c(12)]
bf_M02 <- as.matrix(b_M02_bac_family_df)

b_M03_bac_family_df <- bacteria_family_df[,c(10)]
bf_M03 <- as.matrix(b_M03_bac_family_df)

b_M04_bac_family_df <- bacteria_family_df[,c(19)]
bf_M04 <- as.matrix(b_M04_bac_family_df)

b_M05_bac_family_df <- bacteria_family_df[,c(15)]
bf_M05 <- as.matrix(b_M05_bac_family_df)

b_M06_bac_family_df <- bacteria_family_df[,c(16)]
bf_M06 <- as.matrix(b_M06_bac_family_df)

b_M07_bac_family_df <- bacteria_family_df[,c(13)]
bf_M07 <- as.matrix(b_M07_bac_family_df)

b_M08_bac_family_df <- bacteria_family_df[,c(14)]
bf_M08 <- as.matrix(b_M08_bac_family_df)

b_M09_bac_family_df <- bacteria_family_df[,c(8)]
bf_M09 <- as.matrix(b_M09_bac_family_df)

b_M10_bac_family_df <- bacteria_family_df[,c(9)]
bf_M10 <- as.matrix(b_M10_bac_family_df)

## ===== ##
## 'weights' can be negative
## So try to solve giving only NON-NEGATIVE weights via non-negative least-squares (NNLS)
## see: 'nnls' from https://cran.r-project.org/web/packages/nnls/nnls.pdf
## ===== ##

## ===== ##
## FIRST: Inspect the 'Residual Sum of Squares' [RSS] values
## ===== ##

soln_M01 <- nnls(bacteria_family_matrix_A,bf_M01)
soln_M02 <- nnls(bacteria_family_matrix_A,bf_M02)
soln_M03 <- nnls(bacteria_family_matrix_A,bf_M03)
soln_M04 <- nnls(bacteria_family_matrix_A,bf_M04)
soln_M05 <- nnls(bacteria_family_matrix_A,bf_M05)
soln_M06 <- nnls(bacteria_family_matrix_A,bf_M06)
soln_M07 <- nnls(bacteria_family_matrix_A,bf_M07)
soln_M08 <- nnls(bacteria_family_matrix_A,bf_M08)
soln_M09 <- nnls(bacteria_family_matrix_A,bf_M09)
soln_M10 <- nnls(bacteria_family_matrix_A,bf_M10)

solution <- cbind(soln_M01, soln_M02, soln_M03, soln_M04, soln_M05, soln_M06, soln_M07, soln_M08, soln_M09, soln_M10)

solution[2,]      ### Row 2 holds the values for the 'deviance', or 'Residual Sum of Squares' [RSS] values,
                 ### that is the 'distance' of the solution vector from the projected vector, b

## ===== ##
## SECOND: Grab the solution 'weight' values, or 'X' from [A.X = b]
## pass matrix 'A' and each vector 'b' in turn to the NNLS function
## ===== ##

library("limSolve")
packageVersion("limSolve")

soln_M01 <- nnls(bacteria_family_matrix_A,bf_M01, verbose = TRUE)
soln_M02 <- nnls(bacteria_family_matrix_A,bf_M02, verbose = TRUE)
soln_M03 <- nnls(bacteria_family_matrix_A,bf_M03, verbose = TRUE)
soln_M04 <- nnls(bacteria_family_matrix_A,bf_M04, verbose = TRUE)
soln_M05 <- nnls(bacteria_family_matrix_A,bf_M05, verbose = TRUE)
soln_M06 <- nnls(bacteria_family_matrix_A,bf_M06, verbose = TRUE)
soln_M07 <- nnls(bacteria_family_matrix_A,bf_M07, verbose = TRUE)
soln_M08 <- nnls(bacteria_family_matrix_A,bf_M08, verbose = TRUE)
soln_M09 <- nnls(bacteria_family_matrix_A,bf_M09, verbose = TRUE)
soln_M10 <- nnls(bacteria_family_matrix_A,bf_M10, verbose = TRUE)

solution <- cbind(soln_M01$X, soln_M02$X, soln_M03$X, soln_M04$X, soln_M05$X, soln_M06$X, soln_M07$X, soln_M08$X, soln_M09$X, soln_M10$X)

## name columns and rows ##

```

```
#####
dimnames(solution) = list( c("P1","P4","P5","P8","P9","P10","P12","P13","P15"),c("M1","M2","M3","M4","M5","M6","M7","M8","M9","M10") )

solution ## view the solution 'weights' for each mixed sample

write.table(solution, sep="\t", "solutionWeights.txt")

## ===== ##
## THIRD: plot out the 'weights'
## Plot the weight of contribution for each of the single 'seed' samples to a mixture
## ===== ##

## view weights for each mixed sample as barcharts ##
## munge solution vectors into one vector ##
## the following was adapted from: http://www.r-bloggers.com/using-the-svd-to-find-the-needle-in-the-haystack/ ##

library(lattice)
b_clr <- c("steelblue", "darkred")
b1 <- barchart(as.table(solution[,1]),
  main="M_01",
  horizontal=FALSE, col=ifelse(solution[,1] > 0,
    b_clr[1], b_clr[2]),
  ylab="Weight",
  scales=list(x=list(rot=55, labels=rownames(solution), cex=1.1)),
  ) ###key = key)
print(b1, split=c(1,1,3,4), more=TRUE) ### 'split' is used to lay out the barchart lattice
### e.g. split=c(1,1,3,2) means place plot b1 in col. 1, row 1

b2 <- barchart(as.table(solution[,2]),
  main="M_02",
  horizontal=FALSE, col=ifelse(solution[,2] > 0,
    b_clr[1], b_clr[2]),
  ylab="Weight",
  scales=list(x=list(rot=55, labels=rownames(solution), cex=1.1)),
  ) ###key = key)
print(b2, split=c(2,1,3,4), more=TRUE) ### 'split' is used to lay out the barchart lattice
### e.g. split=c(2,1,3,2) means place plot b2 in col. 2, row 1
### where the layout has 3 columns and 2 rows x O x
### x x x

b3 <- barchart(as.table(solution[,3]),
  main="M_03",
  horizontal=FALSE, col=ifelse(solution[,3] > 0,
    b_clr[1], b_clr[2]),
  ylab="Weight",
  scales=list(x=list(rot=55, labels=rownames(solution), cex=1.1)),
  ) ###key = key)
print(b3, split=c(3,1,3,4), more=TRUE)

b4 <- barchart(as.table(solution[,4]),
  main="M_04",
  horizontal=FALSE, col=ifelse(solution[,4] > 0,
    b_clr[1], b_clr[2]),
  ylab="Weight",
  scales=list(x=list(rot=55, labels=rownames(solution), cex=1.1)),
  ) ###key = key)
print(b4, split=c(1,2,3,4), more=TRUE)

b5 <- barchart(as.table(solution[,5]),
  main="M_05",
  horizontal=FALSE, col=ifelse(solution[,5] > 0,
    b_clr[1], b_clr[2]),
  ylab="Weight",
  scales=list(x=list(rot=55, labels=rownames(solution), cex=1.1)),
  ) ###key = key)
print(b5, split=c(2,2,3,4), more=TRUE)

b6 <- barchart(as.table(solution[,6]),
  main="M_06",
  horizontal=FALSE, col=ifelse(solution[,6] > 0,
    b_clr[1], b_clr[2]),
  ylab="Weight",
  scales=list(x=list(rot=55, labels=rownames(solution), cex=1.1)),
  ) ###key = key)
print(b6, split=c(3,2,3,4), more=TRUE)

b7 <- barchart(as.table(solution[,7]),
  main="M_07",
  horizontal=FALSE, col=ifelse(solution[,7] > 0,
    b_clr[1], b_clr[2]),
  ylab="Weight",
  scales=list(x=list(rot=55, labels=rownames(solution), cex=1.1)),
  ) ###key = key)
print(b7, split=c(1,3,3,4), more=TRUE)

b8 <- barchart(as.table(solution[,8]),
  main="M_08",
```

```

horizontal=FALSE, col=ifelse(solution[,8] > 0,
                             b_clr[1], b_clr[2]),
ylab="Weight",
scales=list(x=list(rot=55, labels=rownames(solution), cex=1.1)),
) ###key = key)
print(b8, split=c(2,3,3,4), more=TRUE)

b9 <- barchart(as.table(solution[,9]),
              main="M_09",
              horizontal=FALSE, col=ifelse(solution[,9] > 0,
                                           b_clr[1], b_clr[2]),
              ylab="Weight",
              scales=list(x=list(rot=55, labels=rownames(solution), cex=1.1)),
              ) ###key = key)
print(b9, split=c(3,3,3,4), more=TRUE)

b10 <- barchart(as.table(solution[,10]),
                main="M_10",
                horizontal=FALSE, col=ifelse(solution[,10] > 0,
                                             b_clr[1], b_clr[2]),
                ylab="Weight",
                scales=list(x=list(rot=55, labels=rownames(solution), cex=1.1)),
                ) ###key = key)
print(b10, split=c(1,4,3,4))

```

Method S1: Code for the Non-Negative Least Squares (NNLS) analysis related to STAR Methods. This annotated code can be run using R in order to obtain the contribution of individual communities towards the community mix. The input files needed are the .biom file containing the compositions of communities analysed and their phylogeny, preferably prepared using Cumulative Sum Scaling normalisation (see STAR methods). It also requires a mapping file as described in http://qiime.org/documentation/file_formats.html. The version of the code is suited for analysis of our dataset but can be readily adapted for any dataset containing multiple communities amplicon data.

The script was run in RStudio v1.0.143 using R version 3.4.0 (2017-04-21) and the following R package versions: limSolve_1.5.5.2, nnls_1.4, biomformat_1.4.0, Phyloseq_1.20.0.